Hindawi Publishing Corporation
Mathematical Problems in Engineering
Volume 2016, Article ID 8048905, 9 pages
http://dx.doi.org/10.1155/2016/8048905

Research Article

A New Double Sliding Mode Observer for EV Lithium Battery SOC Estimation

Qiaoyan Chen,[1,2] Jiuchun Jiang,[1,2] Haijun Ruan,[1,2] and Caiping Zhang[1,2]

[1]*National Active Distribution Network Technology Research Center (NANTEC), School of Electrical Engineering, Beijing Jiaotong University, Beijing 100044, China*
[2]*Collaborative Innovation Center of Electric Vehicles in Beijing, Beijing 100044, China*

Correspondence should be addressed to Qiaoyan Chen; tianjincqy@163.com

Received 17 April 2016; Accepted 6 September 2016

Academic Editor: Xiangyu Meng

A new sliding mode observer is proposed in this paper; compared with the existing sliding mode observer used for SOC estimation, the new observer has the advantages of simple design and good generality. The robustness of the new observer was proved by Lyapunov stability theorem. Taking the first-order Randle circuit model of the battery as an example, the new sliding mode observer was designed. Battery test was done with the simulated FUDS condition, and the robustness of the new observer was verified by the test. Because battery internal ohmic resistance is changing in battery working process, which has a significant effect on SOC estimation, a new double sliding mode observer was designed to identify the internal resistance. The tests results show that the battery internal ohmic resistance changes greatly when the SOC is low and the double observer can accurately identify the resistance which improves the accuracy of the battery model. The results also show that the new double observer is robust and can improve the precision of SOC estimation when the battery remaining capacity is low.

1. Introduction

For the requirements of energy saving, environmental protection, and the industrial upgrading, electric vehicles (EVs) have become a new development direction of automobile industry. The lithium battery has the advantages of high energy density, high power density, long cycle life, and so on, so it has become the main storage component of EVs. The battery management system (BMS) has the functions of maintaining safe and reliable battery and giving full potential of battery performance, and state of charge (SOC) estimation is the basis of battery management.

When battery works, there exist complex physical and chemical reactions in the battery, so the battery parameters show strong nonlinear uncertain characteristics, which make it very difficult to estimate the battery SOC. Current integral is a common estimation method, but this method needs to know the initial SOC, and the current measurement error accumulates over time [1, 2]. The modeling method is designing battery electrochemical model and analyzing the parameters for SOC estimation, and this method involves multiple parameters' analysis, fitting, and calculation [3]. Electrochemical impedance spectrum (EIS) analysis needs an external multifrequency excitation source [4, 5]. The estimation accuracy of Kalman filter relies on battery model; however, it is difficult to obtain the noise covariance of the model [6–12]. Neural network requires a large amount of sample data to train the model. The sample data selection and the training methods affect the estimation accuracy [12–16]. Least squares and mathematical fitting are all based on the fitting curves, and the methods are limited by the fitting conditions [17, 18]. Luenberger observer and H infinity observer are nonlinear observers. Luenberger observer lacks robustness and the estimation result is influenced by the uncertain disturbance [19]. H infinity observer is robust, but the design is complex [20, 21].

Sliding mode observer has good robustness and can estimate battery SOC in real time, which is suitable for electric vehicle power battery SOC estimation [22–32]. At present, there are mainly two design methods of sliding mode observer: (1) battery state space equation is established in matrix form, and the observer is designed for the whole

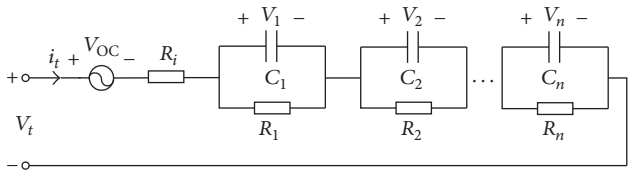

Figure 1: The battery nth-order Randle circuit model.

state vector estimation [22–25]. This method requires solving matrix equations, so the design is complex. (2) Battery state space equation is established in the form of equations, and the observers are designed for each state component of the state vector estimation [26–32]. This method needs to design multiple observers, so the design is complex and particularly the equation group dimension is higher.

A new sliding mode observer is proposed in this paper. The new sliding mode observer neither requires solving matrix equations nor requires designing multiple observers, and the observer design is simple. The robustness of the new sliding mode observer was proved by Lyapunov stability theory. Because the battery internal ohmic resistance changes greatly when the SOC is low and the changing has significant impact on SOC estimation, a new double sliding mode observer was designed to identify the internal ohmic resistance, and the model parameter was updated in real time, which improves the accuracy of battery model.

The nth-order Randle circuit model was chosen to establish battery state space equation. Based on the model, a new observer was designed for SOC estimation. The design processes showed that the new observer is simple and generally applicable. In order to verify the performance of the new observer, a nominal capacity of 25 AH lithium battery was chosen as the test object. The test was operated with the simulated FUDS cycles, and the designed new sliding mode observer, based on first-order Randle model, was used to estimate the SOC with the test data. The estimation results showed that the new sliding mode observer is robust. A new double sliding mode observer was designed to identify the battery internal ohmic resistance and to estimate the SOC. The tests results showed that the new double sliding mode observer can accurately identify the internal ohmic resistance and also showed that the internal ohmic resistance changes greatly when the battery runs low, and the new double sliding mode observer improved the precision of SOC estimation when the battery residual capacity is low.

2. Battery Modeling

2.1. Battery Modeling. State space equation of the battery nth-order Randle circuit model is simple and regular, so the circuit model was chosen to establish battery state space equation. The nth-order Randle circuit model is shown in Figure 1 [33], where V_{OC} is the open circuit voltage (OCV) and there exists a function relationship $V_{OC} = g(\text{SOC})$ between V_{OC} and the battery SOC; R_i is the internal ohmic resistance; $C_1, C_2, \ldots, C_n$ and $R_1, R_2, \ldots, R_n$ reflect the charge transfer and diffusion effect; i_t is the battery input current; and V_t is the battery terminal voltage.

Choosing $[V_1, V_2, \ldots, V_n, V_{OC}]^T$ as state vector, assuming the battery capacity is Q_n, and considering the influence of linearization error, the errors caused by battery internal and external disturbances, and so on, the nth-order Randle circuit model state space equation can be expressed as

$$\begin{bmatrix} \dot{V}_1 \\ \dot{V}_2 \\ \vdots \\ \dot{V}_n \\ \dot{V}_{OC} \end{bmatrix} = \operatorname{diag}\left(-\frac{1}{R_1C_1}, -\frac{1}{R_2C_2}, \ldots, -\frac{1}{R_nC_n}, 0\right) \begin{bmatrix} V_1 \\ V_2 \\ \vdots \\ V_n \\ V_{OC} \end{bmatrix} + \begin{bmatrix} \frac{1}{C_1} \\ \frac{1}{C_2} \\ \vdots \\ \frac{1}{C_n} \\ \frac{dg(s)/ds}{Q_n} \end{bmatrix} i_t + \begin{bmatrix} f_1 \\ f_2 \\ \vdots \\ f_n \\ f_{n+1} \end{bmatrix}, \quad (1)$$

where $f_1, f_2, \ldots, f_n$ are the sum of all the above errors, which are bounded, nonlinear, and uncertain functions. The battery observation equation is expressed as

$$V_t = [1, 1, \ldots, 1]\left[V_1, V_2, \ldots, V_n, V_{OC}\right]^T + R_i i_t. \quad (2)$$

Equations (1) and (2) are battery state space equation, where state vector $\mathbf{x} = [V_1, V_2, \ldots, V_n, V_{OC}]^T$, observation $\mathbf{y} = V_t$, and the coefficient matrixes of the system are $\mathbf{A} = \operatorname{diag}(-1/R_1C_1, -1/R_2C_2, \ldots, -1/R_nC_n, 0)$, $\mathbf{B} = [1/C_1, 1/C_2, \ldots, 1/C_n, 1/Q_n]^T$, and $\mathbf{C} = [1, 1, \ldots, 1]$, $\mathbf{D} = R_i$. The circuit model is Thevenin circuit model when $n = 1$, and it is 2nd-order circuit model when $n = 2$.

In battery working process, the battery internal ohmic resistance is changing, and the changing resistance can be expressed as [26]

$$R_i(t) = R_i(0) + \theta t + \delta, \quad (3)$$

where $R_i(t)$ is the time-varying battery internal ohmic resistance; $R_i(0)$ is the initial ohmic resistance; θ is a constant coefficient; and δ is a bounded, nonlinear, and uncertain

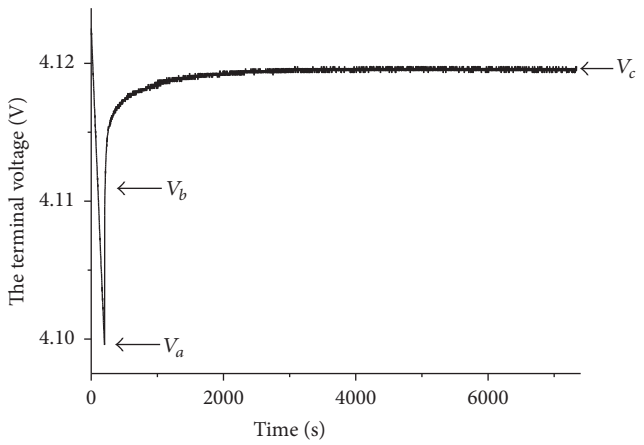

Figure 2: The battery terminal voltage after pulse discharge.

function. By the derivative of (3), the state equation of the internal ohmic resistance can be expressed as [26]

$$\dot{R}_i(t) = \theta + \frac{d\delta}{dt}, \tag{4}$$

where $d\delta/dt$ is a bounded, nonlinear, and uncertain function; θ is taken as 0 in this paper; and (4) and (2) are the state space equations of the internal ohmic resistance.

2.2. Battery Model Parameters Identification. The battery circuit model parameters values can be obtained through pulse discharge. When the battery SOC = 94.9%, battery terminal voltage curve after pulse discharge is shown in Figure 2.

From Figures 1 and 2, it can be seen that the ohmic internal resistance of circuit model can be expressed as

$$R_i = \frac{V_b - V_a}{\Delta i_t}. \tag{5}$$

n RC branch time constants of circuit model are $\tau_1 = R_1C_1, \tau_2 = R_2C_2, \ldots, \tau_n = R_nC_n$. Battery terminal voltage after pulse discharge can be given as

$$V_t = V_b + iR_1\left(1 - e^{(-t/\tau_1)}\right) + iR_2\left(1 - e^{(-t/\tau_2)}\right) + \cdots + iR_n\left(1 - e^{(-t/\tau_n)}\right). \tag{6}$$

The sum of the branch resistances can be expressed as

$$R_1 + R_2 + \cdots + R_n = \frac{V_c - V_b}{\Delta i_t}. \tag{7}$$

According to (6) and (7), n time constants $\tau_1, \tau_2, \ldots, \tau_n$ and n branch resistances $R_1, R_2, \ldots, R_n$ can be obtained by least squares method.

The first-order Randle circuit model is Thevenin circuit model. After pulse discharge, 200 sampling points were chosen to identify the parameters of the model with least squares method. The parameters of Thevenin circuit model are shown in Table 1.

Table 1: The parameters of Thevenin circuit model.

Parameters	R_i (mΩ)	R_1 (mΩ)	C_1 (F)	Q_n (C)
Values	1.12	1.26	7.78×10^4	9.67×10^4

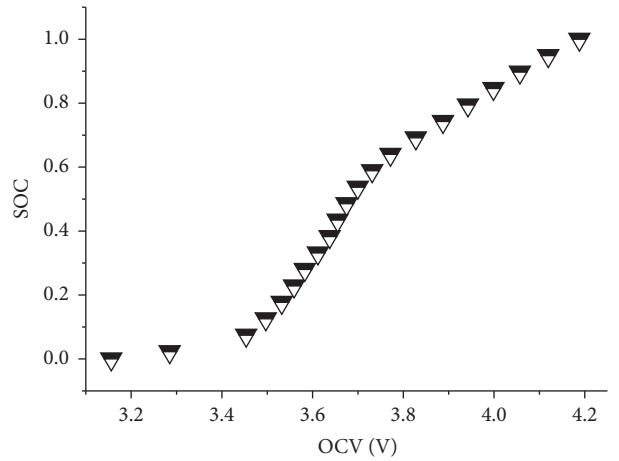

Figure 3: SOC versus OCV.

2.3. The Function of the SOC versus OCV. There exists a function relationship between SOC and OCV, which can be got by measurement and mathematical fitting method. Taking OCV as independent variable, the function of SOC versus OCV SOC = $g^{-1}(V_{OC})$ is shown in Figure 3.

The estimation results of the new observer are OCV and terminal voltages of all the RC parallel branches and SOC estimation can be got according to the function of SOC versus OCV.

3. Design of the New Double Sliding Mode Observer

3.1. The New Sliding Mode Observer. Assume the nonlinear uncertain system is modeled by the following equations:

$$\begin{aligned} \dot{\mathbf{x}}(\mathbf{t}) &= \mathbf{A}\mathbf{x}(\mathbf{t}) + \mathbf{B}\mathbf{u}(\mathbf{t}) + \mathbf{f}(\mathbf{x}, \mathbf{u}, \mathbf{t}), \\ \mathbf{y}(\mathbf{t}) &= \mathbf{C}\mathbf{x}(\mathbf{t}) + \mathbf{D}\mathbf{u}(\mathbf{t}), \end{aligned} \tag{8}$$

where $\mathbf{A} \in R^{n\times n}$, $\mathbf{B} \in R^{n\times m}$, $\mathbf{C} \in R^{l\times n}$, and $\mathbf{D} \in R^{l\times m}$ are coefficient matrixes, $\mathbf{u}(t) \in R^m$ is the control variable, $\mathbf{B}$ and $\mathbf{C}$ are full rank, $(\mathbf{A}, \mathbf{C})$ is observable, and $\mathbf{f}(\mathbf{x}, \mathbf{u}, \mathbf{t}) = [f_1, f_2, \ldots, f_n]^T \in R^n$ is a bounded uncertain nonlinear function. For system (8), the observer is designed as [34]

$$\dot{\hat{\mathbf{x}}}(\mathbf{t}) = \mathbf{A}\hat{\mathbf{x}}(\mathbf{t}) + \mathbf{B}\mathbf{u}(\mathbf{t}) - \mathbf{G}\left(\hat{\mathbf{y}}(\mathbf{t}) - \mathbf{y}(\mathbf{t})\right) + \mathbf{B}\mathbf{v}, \tag{9}$$

where $\hat{\mathbf{x}}(\mathbf{t}) \in R^n$ is the system state estimation, $\mathbf{G} \in R^{n\times l}$ is the designed matrix, and $\mathbf{v}(\hat{\mathbf{x}}, \mathbf{t}) \in R^n \times R^+ \to R^n$ is the designed control variable of the observer. Assume the system state estimation error is $\mathbf{e}(\mathbf{t}) = \hat{\mathbf{x}}(\mathbf{t}) - \mathbf{x}(\mathbf{t})$. From (8) and (9), the error system can be expressed as

$$\dot{\mathbf{e}}(\mathbf{t}) = \mathbf{A}_0\mathbf{e}(\mathbf{t}) - \mathbf{f}(\mathbf{x}, \mathbf{u}, \mathbf{t}) + \mathbf{B}\mathbf{v}, \tag{10}$$

where $\mathbf{A}_0 = \mathbf{A} - \mathbf{GC}$. The sliding mode surface is designed as

$$\mathbf{S} = \mathbf{F}\left(\hat{\mathbf{y}}(\mathbf{t}) - \mathbf{y}(\mathbf{t})\right) = \mathbf{FC}\left(\hat{\mathbf{x}}(\mathbf{t}) - \mathbf{x}(\mathbf{t})\right) = \mathbf{Me} = 0. \quad (11)$$

The control variable is designed as

$$\mathbf{v} = \begin{cases} -\rho \dfrac{\left(\mathbf{S}^T\mathbf{MB}\right)^T}{\left\|\mathbf{S}^T\mathbf{MB}\right\|^2} \|\mathbf{S}\| \|\mathbf{MB}\| & \left\|\mathbf{S}^T\mathbf{MB}\right\| \neq 0 \\ 0 & \left\|\mathbf{S}^T\mathbf{MB}\right\| = 0. \end{cases} \quad (12)$$

Block matrix form of error system can be written as

$$\begin{aligned} \dot{\mathbf{e}}_1(\mathbf{t}) &= \mathbf{A}_{011}\mathbf{e}_1(\mathbf{t}) + \mathbf{A}_{012}\mathbf{e}_2(\mathbf{t}) + \mathbf{f}_1 + \mathbf{B}_1\mathbf{v}, \\ \dot{\mathbf{e}}_2(\mathbf{t}) &= \mathbf{A}_{021}\mathbf{e}_1(\mathbf{t}) + \mathbf{A}_{022}\mathbf{e}_2(\mathbf{t}) + \mathbf{f}_2 + \mathbf{B}_2\mathbf{v}. \end{aligned} \quad (13)$$

The block matrixes are $\mathbf{A}_0 = \begin{bmatrix} \mathbf{A}_{011}{}^{(n-1)\times(n-1)} & \mathbf{A}_{012}{}^{(n-1)\times 1} \\ \mathbf{A}_{021}{}^{1\times(n-1)} & \mathbf{A}_{022}{}^{1\times 1} \end{bmatrix}$, $\mathbf{B} = [\mathbf{B}_1{}^{(n-1)\times m}; \mathbf{B}_2{}^{1\times m}]$, $\mathbf{f} = [\mathbf{f}_1{}^{(n-1)\times 1}; \mathbf{f}_2{}^{1\times 1}]$. The corresponding block matrix form of sliding surface can be written as

$$\mathbf{S} = \mathbf{Me} = \mathbf{M}_1\mathbf{e}_1 + \mathbf{M}_2\mathbf{e}_2 = 0. \quad (14)$$

Meeting the following two assumptions, the observer is robust:

(1) $\mathbf{A}_{011}$ is Hurwitz matrix, and the last column of $\mathbf{A}_0$ is zero vector, which is $\mathbf{A}_{012} = 0$ and $\mathbf{A}_{022} = 0$.

(2) $\rho\|\mathbf{MB}\| \geq \|\mathbf{Mf}\|$.

3.2. Convergence Proof of the New Observer. Lyapunov function is chosen as

$$V = \frac{1}{2}\mathbf{S}^T\dot{\mathbf{S}} = \frac{1}{2}\|\mathbf{S}\|^2 \geq 0. \quad (15)$$

Then,

$$\begin{aligned} \dot{V} &= \mathbf{S}^T\dot{\mathbf{S}} = \mathbf{e}^T\mathbf{M}^T\mathbf{M}\dot{\mathbf{e}} = \mathbf{e}^T\mathbf{M}^T\mathbf{M}\left(\mathbf{A}_0\mathbf{e} - \mathbf{f} + \mathbf{Bv}\right) \\ &= \mathbf{e}^T\mathbf{M}^T\mathbf{MA}_0\mathbf{e} - \mathbf{S}^T\mathbf{Mf} + \mathbf{S}^T\mathbf{MBv} \\ &\leq \lambda_{\max}\left(\mathbf{M}^T\mathbf{MA}_0\right)\|e\|^2 - \mathbf{S}^T\mathbf{Mf} + \mathbf{S}^T\mathbf{MBv}. \end{aligned} \quad (16)$$

Because $\mathbf{M}^T\mathbf{M} = \|\mathbf{F}\|^2\|\mathbf{C}\|^2 \geq 0$ and $\lambda_{\max}(\mathbf{A}_0) \leq 0$

$$\dot{V} \leq \|\mathbf{S}\| \|\mathbf{Mf}\| + \mathbf{S}^T\mathbf{MBv} = \|\mathbf{S}\| \|\mathbf{Mf}\| - \rho\|\mathbf{S}\| \|\mathbf{MB}\|. \quad (17)$$

If $\rho\|\mathbf{MB}\| > \|\mathbf{Mf}\|$ and $\mathbf{S} \neq 0$, then $\dot{V} < 0$.

Therefore, the state variable converges to the sliding mode surface.

From (11) and (12), it can be seen that the control variable $\mathbf{v} = 0$ on the sliding mode surface. The error system linear row transformation does not change the convergence of the system. With the transformation of (13) and for $\mathbf{A}_{021} = 0$ and $\mathbf{A}_{022} = 0$, the error system can be expressed as

$$\begin{aligned} \dot{\mathbf{e}}_1(\mathbf{t}) &= \mathbf{A}'_{011}\mathbf{e}_1(\mathbf{t}) + \mathbf{B}_1\mathbf{v}, \\ \dot{\mathbf{e}}_2(\mathbf{t}) &= \mathbf{f}'_2 + \mathbf{B}_2\mathbf{v}, \end{aligned} \quad (18)$$

where $\mathbf{A}'_{011}$ is the linear row transformation result of $\mathbf{A}_{011}$. $\mathbf{A}_{011}$ is a Hurwitz matrix, so $\mathbf{A}'_{011}$ is also a Hurwitz matrix, and so $\mathbf{e}_1(\mathbf{t})$ converges to zero-equilibrium point. According to (14), $\mathbf{e}_2(\mathbf{t})$ can be expressed as

$$\mathbf{e}_2 = -\mathbf{M}_2^{-1}\mathbf{M}_1\mathbf{e}_1. \quad (19)$$

Therefore, $\mathbf{e}_2(\mathbf{t})$ also converges to zero-equilibrium point, as a result, $\mathbf{e}(\mathbf{t})$ converges to zero-equilibrium point, and the convergence speed is related to the eigenvalue of $\mathbf{A}_{011}$. For the system is an uncertain system, the convergence of the new observer is robust.

3.3. Design of the New Double Sliding Mode Observer. According to state equations (1) and (2), the discrete form of the new sliding mode observer is expressed as

$$\begin{aligned} \hat{\mathbf{y}}(\mathbf{k-1}) &= \mathbf{C}\hat{\mathbf{x}}(\mathbf{k-1}) + \hat{R}_i(k-1)\,I(k); \\ \mathbf{S}(\mathbf{k}) &= \mathbf{M}\left(\hat{\mathbf{x}}(\mathbf{k-1}) - \mathbf{x}(\mathbf{k})\right) \\ &= \mathbf{F}\left(\hat{\mathbf{y}}(\mathbf{k-1}) - \mathbf{y}(\mathbf{k})\right), \end{aligned} \quad (20)$$

where $\mathbf{M} = \mathbf{FC}$,

$$\mathbf{v}(\mathbf{k}) = \begin{cases} -\rho \dfrac{\left(\mathbf{S}(\mathbf{k})^T\mathbf{MB}\right)^T}{\left\|\mathbf{S}(\mathbf{k})^T\mathbf{MB}\right\|^2} \|\mathbf{S}(\mathbf{k})\| \|\mathbf{MB}\| & \left\|\mathbf{S}(\mathbf{k})^T\mathbf{MB}\right\| \neq 0 \\ 0 & \left\|\mathbf{S}(\mathbf{k})^T\mathbf{MB}\right\| = 0, \end{cases} \quad (21)$$

$$\begin{aligned} d\hat{\mathbf{x}}(\mathbf{k-1}) &= \mathbf{A}\hat{\mathbf{x}}(\mathbf{k-1}) + \mathbf{Bu}(\mathbf{k}) - \mathbf{G}\left(\mathbf{C}\hat{\mathbf{x}}(\mathbf{k-1}) - \mathbf{y}(\mathbf{k})\right) \\ &\quad + \mathbf{Bv}(\mathbf{k}), \end{aligned} \quad (22)$$

$$\hat{\mathbf{x}}(\mathbf{k}) = \hat{\mathbf{x}}(\mathbf{k-1}) + d\hat{\mathbf{x}}(\mathbf{k-1}) \cdot \Delta t. \quad (23)$$

The open circuit voltage $V_{\mathrm{OC}}(k)$ is the component of state vector $\mathbf{x}(\mathbf{k})$, so the open circuit voltage estimation $\widehat{V}_{\mathrm{OC}}(k)$ also can be obtained. Battery SOC estimation can be got through the function of SOC versus OCV, and it is given as

$$\widehat{S}_{\mathrm{OC}}(k) = g\left[\widehat{V}_{\mathrm{OC}}(k)\right]. \quad (24)$$

We design $\mathbf{G} = [\mathbf{0}, \mathbf{0}, \ldots, \mathbf{0}]^T$, and, according to $\mathbf{A}_0 = \mathbf{A} - \mathbf{GC}$, then $\mathbf{A}_0 = \mathbf{A} = \mathrm{diag}[-1/R_1C_1, -1/R_2C_2, \ldots, -1/R_nC_n, 0]$, which meets assumption (1). According to the test, we design $\rho > 10$, which can meet assumption (2). From the design processes, it can be seen that the new observer design is simple.

The new observer also can be used in the other battery models for SOC estimation. As long as the coefficient matrixes of battery models meet the two assumptions of the new observer, the new sliding mode observer, based on the models, can be designed as (20)–(24); therefore the new observer is generally applicable.

Based on internal ohmic resistance state equations (4) and (2), the discrete form of the sliding mode observer for the resistance is designed as [26]

$$\dot{\hat{R}}_i(t) = \theta_c + L\,\mathrm{sgn}\left(R_i(t) - \hat{R}_i(t)\right), \quad (25)$$

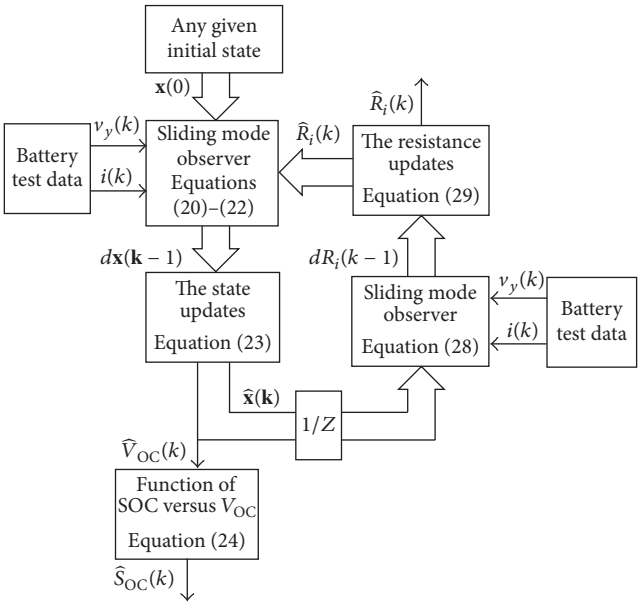

Figure 4: The whole algorithm of the new double sliding mode observer.

where L is the designed parameter. According to (3), the observer can be expressed as

$$\dot{R}_i(t) = \theta_c + L\,\mathrm{sgn}\left(y(t) - \frac{\widehat{y}(t)}{i(t)}\right). \tag{26}$$

According to (4) and (26), the state equation of error system can be expressed as [26]

$$\dot{e}_R = \xi - L\,\mathrm{sgn}\left(y(t) - \frac{\widehat{y}(t)}{i(t)}\right). \tag{27}$$

If $L > |\xi|$, then $\dot{e}_R < 0$, and the error of internal ohmic resistance e_R converges to zero.

The discrete form of the observer for internal ohmic resistance estimation is expressed as

$$\begin{aligned} \widehat{\mathbf{y}}(\mathbf{k}) &= \mathbf{C}\hat{\mathbf{x}}(\mathbf{k}) + \widehat{R}_i(k-1)\,I(k); \\ d\widehat{R}_i(k-1) &= L\,\mathrm{sgn}\left(y(k) - \frac{\widehat{y}(k)}{i(k)}\right), \end{aligned} \tag{28}$$

$$\widehat{R}_i(k) = \widehat{R}_i(k-1) + d\widehat{R}_i(k-1)\,\Delta t. \tag{29}$$

Equations (20)–(24), (28), and (29) are the new double sliding mode observer, and the estimation results of the observer are SOC, internal ohmic resistance, and terminal voltage of all the RC parallel branches. Figure 4 is the schematic diagram of the new double sliding mode observer.

4. The Experimental Verification

4.1. The Battery Testing Platform. In order to verify the performance of the new dual sliding mode observer, a 25 AH nominal capacity lithium ion power battery was tested under simulation conditions; the battery is shown in Figure 5.

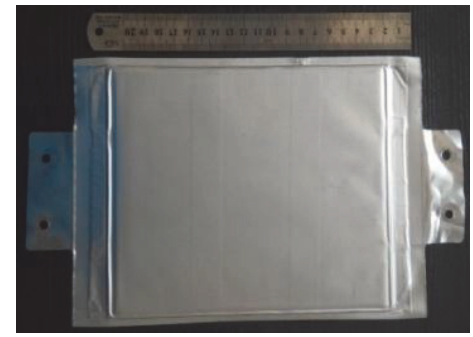

Figure 5: The 25 AH nominal capacity lithium ion power battery.

(a) The Arbin BT2000 (b) The thermostat

Figure 6: The battery testing equipment.

Battery testing platform consists of Arbin BT2000 battery testing system which is shown in Figure 6(a), thermostat which is shown in Figure 6(b), host computer, and the corresponding monitoring software. The battery testing system is controlled by the host computer and has battery charge and discharge functions. The monitoring software has the function of setting battery working conditions. The host computer can collect, monitor, and store battery experimental data in real time. The thermostat maintains the battery external environment temperature.

4.2. SOC Estimation with the New Sliding Mode Observer. The test battery, shown in Figure 5, was put into the incubator, in which the temperature was 20°C, for two hours, and was repeatedly charged and discharged in order to activate it and then was charged to SOC = 100%. Because the simulated FUDS condition includes charge and discharge processes, to avoid the battery being overcharged, firstly it was discharged for 1 AH with $C/3$ rate and then it was operated under the simulated FUDS drive cycles. When the battery terminal voltage reaches 3 V cut-off voltage, the test was stopped. Battery test platform can measure and store battery current and terminal voltage in real time, and the sampling time is

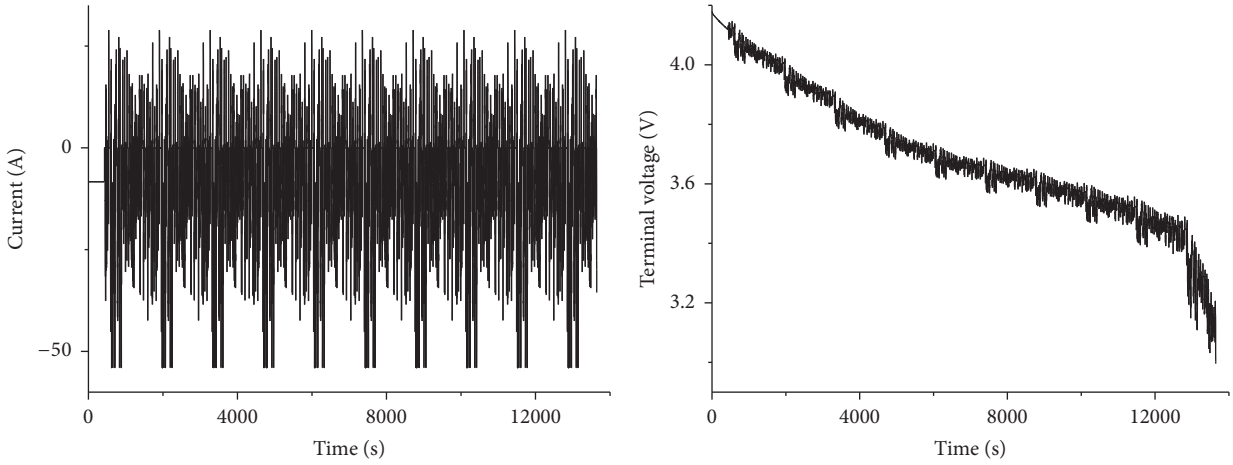

(a) The current of the simulated FUDS condition

(b) The voltage of the simulated FUDS condition

Figure 7: The simulated FUDS condition.

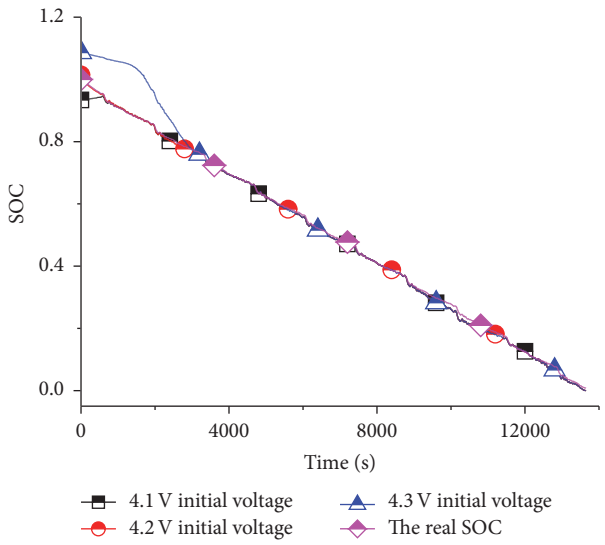

Figure 8: The SOC estimations with the new sliding mode observer.

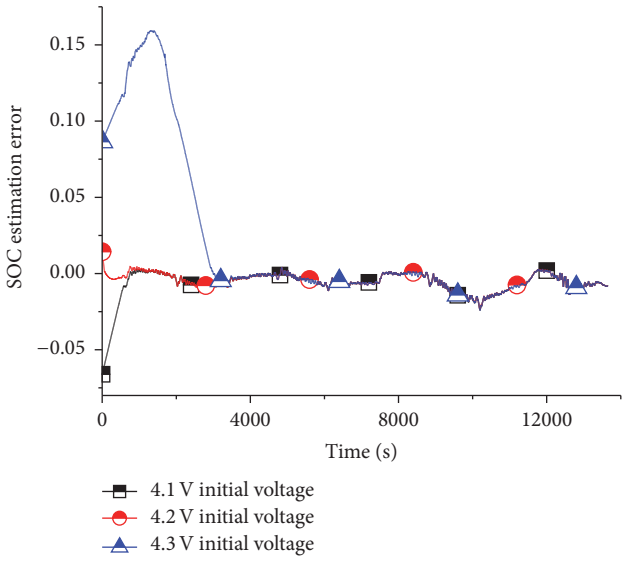

Figure 9: The SOC estimation errors with the new sliding mode observer.

1 second. The battery working current and terminal voltage under the simulated FUDS drive cycles are shown in Figure 7.

If the initial battery SOC is known, the real SOC can be obtained through current integration when the integration time is not too long. The equation of current integration for real SOC calculation is expressed as

$$\mathrm{SOC} = \mathrm{SOC}_0 - \frac{\int_{t_0}^{t} \eta i_t dt}{Q_n}, \tag{30}$$

where SOC_0 is the initial SOC, Q_n is the battery capacity, i_t is the battery current, and η is the current efficiency. i_t and Q_n can be obtained through measurement. The battery residual capacity can be got through open circuit voltage method. In the test, the battery residual capacity is 0.78 AH. The sum of the discharged electricity quantity, calculated with $\eta = 1$, and the residual capacity is almost equal to the battery capacity, so η is taken as 1.

When using the new sliding mode observer and the new double sliding mode observer, the initial state can be set as an arbitrary value within the stable range of the observers. The first-order Randal model observer is used in the paper. We may assume that the initial open circuit voltage V_{OC} is 4.1 V, 4.2 V, and 4.3 V, and the initial polarization voltage is V_p = 0 V, then the initial state vector $\mathbf{x}_0$ is $[0, 4.1]^T$, $[0, 4.2]^T$, and $[0, 4.3]^T$. The estimation results of the new sliding observer are shown in Figure 8, and the corresponding estimation errors are shown in Figure 9.

From Figures 8 and 9, it can be seen that the estimation results of the new observer are not affected by the nonlinear uncertain functions part of the battery state equation, so the

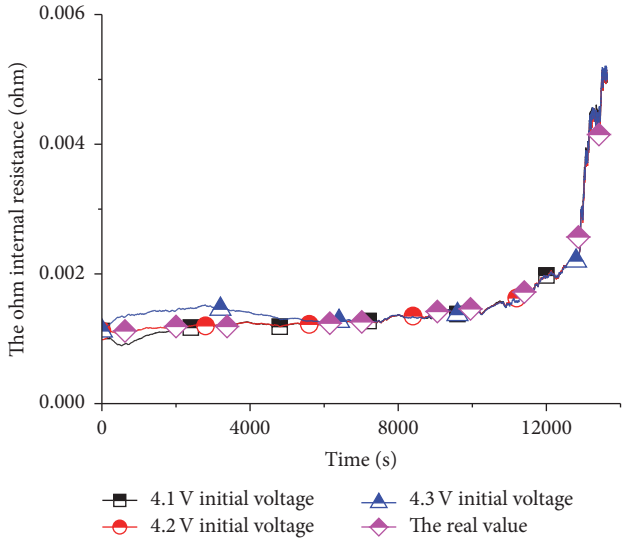

Figure 10: The internal ohmic resistance estimations with the new double sliding mode observer.

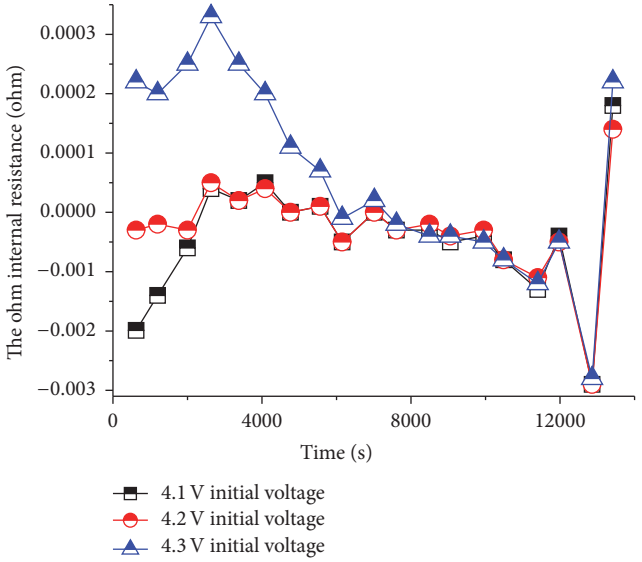

Figure 11: The internal ohmic resistance estimation errors with the new double sliding mode observer.

new sliding mode observer is robust. If the battery initial states are the above values, the maximum estimation error of the new observer is 2.41% when the estimation results are stable. In the observer stable range, almost the same convergence result can be got when choosing the other initial state vectors.

4.3. SOC Estimation with the New Double Sliding Mode Observer. In battery working processes, the internal ohmic resistance is changing over time. The test battery is a power-type battery, and it can be known, through the test, that the discharge current rate has very little impact on the battery internal ohmic resistance [35, 36], so the battery real internal

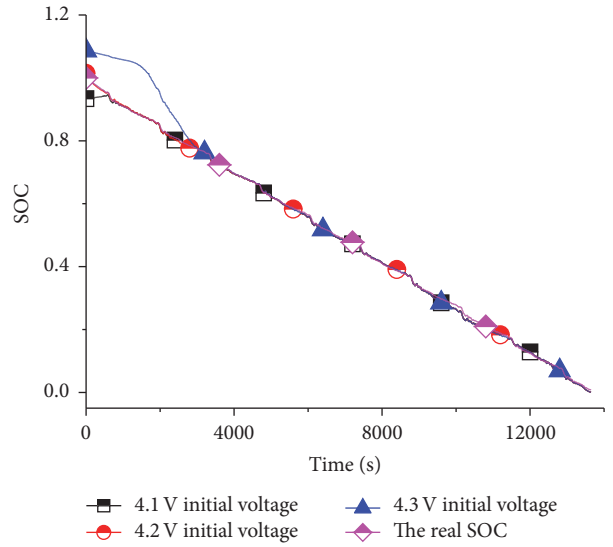

Figure 12: The SOC estimations with the new double sliding mode observer.

ohmic resistance can be obtained through pulse discharge method. At room temperature, the internal ohmic resistance estimations by the new double sliding mode observer and the real values at different SOC values are shown in Figure 10, and the corresponding internal ohmic resistance estimation errors are shown in Figure 11.

From Figures 10 and 11, it can be seen that although the initial states are different, the estimations of the internal ohmic resistance converge to the real value, which improves the accuracy of battery model. When the SOC is low, the estimation errors of the resistance are larger, but the change rate of the open circuit voltage with respect to the SOC is larger too, which reduces the effect of the estimation errors on the SOC estimation.

If the initial state vector $\mathbf{x}_0$ is $[0, 4.1]^T$, $[0, 4.2]^T$, and $[0, 4.3]^T$, the SOC estimations of the new double sliding mode observer are shown in Figure 12, and the corresponding estimation errors are shown in Figure 13.

From Figures 12 and 13, it also can be seen that the new double sliding mode observer is robust. In Figure 13, the maximum estimation error of the new double sliding mode observer is 1.85% when the estimation results are stable.

Assume the initial state is $\mathbf{x}_0 = [0, 4.2]^T$, and the SOC estimation errors of the two observers are shown in Figure 14. Figures 10 and 11 show that the internal ohmic resistance changes greatly at the low SOC. The new double sliding mode observer can identify and update the resistance in real time, which improves the accuracy of the model and the SOC estimation when the SOC is low. Figure 14 shows that the double observer decreases the magnitude of the error and the average error when the SOC is low.

5. Conclusions

(1) A simple design sliding mode observer is proposed in this paper. The robustness of the new observer

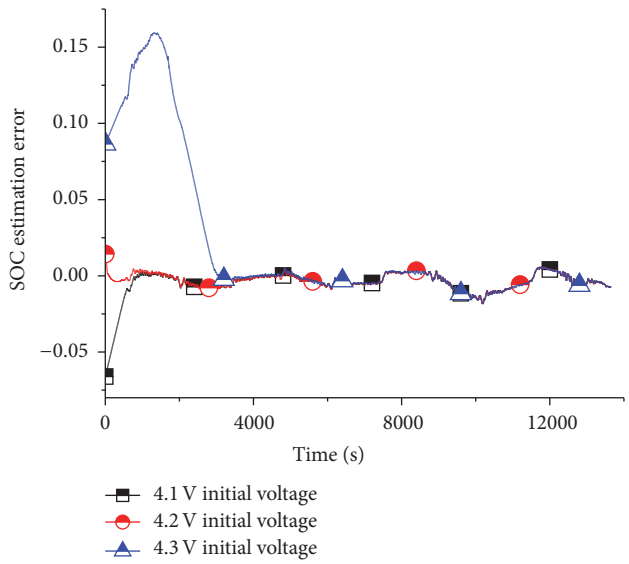

Figure 13: The SOC estimation errors with the new double sliding mode observer.

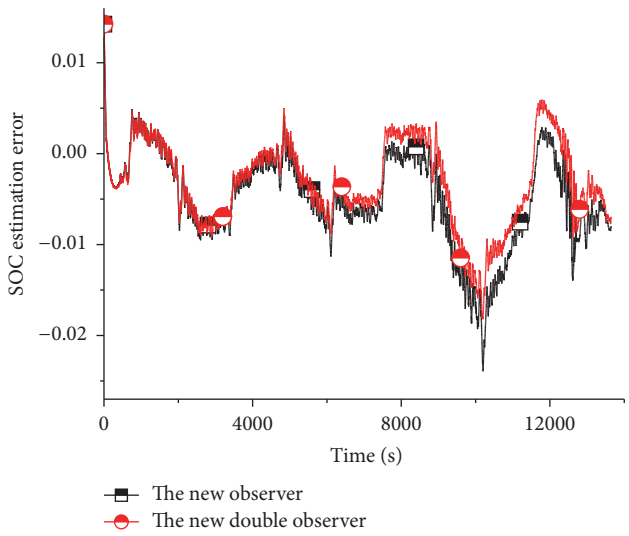

Figure 14: The SOC estimation errors with the two observers.

was proved by Lyapunov's stability theory and the performance of the observer was verified by the simulated FUDS driving condition.

(2) Compared with the new sliding mode observer, the new double sliding mode observer improves the accuracy of battery model and improves the SOC estimation when the battery SOC is low.

(3) The analysis shows that as long as the coefficient matrixes of the battery state equations meet the two assumptions, the observer of the state equations can be designed as the new sliding mode observer in this paper, so it has good generality.

(4) In theory, the other model parameters also can be identified with the new double sliding mode observer, but in practice, for the influences of measurement errors, various interferences, and nonlinear characteristics, they are difficult to be identified if the change of the parameters has no significant impact on the observations.

Competing Interests

The authors declare that there is no conflict of interests regarding the publication of this paper.

Acknowledgments

The work was supported by the National Natural Science Foundation of China (no. 51477009).

References

[1] K. S. Ng, C.-S. Moo, Y.-P. Chen, and Y.-C. Hsieh, "Enhanced coulomb counting method for estimating state-of-charge and state-of-health of lithium-ion batteries," *Applied Energy*, vol. 86, no. 9, pp. 1506–1511, 2009.

[2] J. Wang, B. Cao, Q. Chen, and F. Wang, "Combined state of charge estimator for electric vehicle battery pack," *Control Engineering Practice*, vol. 15, no. 12, pp. 1569–1576, 2007.

[3] J. Marcicki, M. Canova, A. T. Conlisk, and G. Rizzoni, "Design and parametrization analysis of a reduced-order electrochemical model of graphite/$LiFePO_4$ cells for SOC/SOH estimation," *Journal of Power Sources*, vol. 237, pp. 310–324, 2013.

[4] J. H. Jang and J. Y. Yoo, "Impedance-based and circuit-parameter-based battery models for HEV power systems," *International Journal of Automotive Technology*, vol. 9, no. 5, pp. 615–623, 2008.

[5] O. S. Mendoza-Hernandez, H. Ishikawa, Y. Nishikawa, Y. Maruyama, Y. Sone, and M. Umeda, "State of charge dependency of graphitized-carbon-based reactions in a lithium-ion secondary cell studied by electrochemical impedance spectroscopy," *Electrochimica Acta*, vol. 131, pp. 168–173, 2014.

[6] X. Hu, F. Sun, and Y. Zou, "Comparison between two model-based algorithms for Li-ion battery SOC estimation in electric vehicles," *Simulation Modelling Practice and Theory*, vol. 34, pp. 1–11, 2013.

[7] X. Zhang, X. Wang, W. Zhang, and G. Lei, "A simplified Li-ion battery SOC estimating method," *Transactions on Electrical and Electronic Materials*, vol. 17, no. 1, pp. 13–17, 2016.

[8] C. Piao, M. Liu, L. Su, Z. Li, C. Cho, and S. Lu, "Study on stable estimation method for lead-acid battery SOC by extended kalman filter," *International Journal of Control and Automation*, vol. 7, no. 4, pp. 429–438, 2014.

[9] R. Xiong, F.-C. Sun, and H.-W. He, "Data-driven state-of-charge estimator for electric vehicles battery using robust extended Kalman filter," *International Journal of Automotive Technology*, vol. 15, no. 1, pp. 89–96, 2014.

[10] Y. Yin and W. Zhong, "Study on SOC estimation of power battery based on kalman filter optimization algorithm," *International Journal of Hybrid Information Technology*, vol. 8, no. 7, pp. 199–206, 2015.

[11] J. Du, Z. Liu, and Y. Wang, "State of charge estimation for Li-ion battery based on model from extreme learning machine," *Control Engineering Practice*, vol. 26, no. 1, pp. 11–19, 2014.

[12] A. Baba and S. Adachi, "SOC estimation of HEV/EV battery using series kalman filter," *Electrical Engineering in Japan*, vol. 187, no. 2, pp. 53–62, 2014.

[13] L. Kang, X. Zhao, and J. Ma, "A new neural network model for the state-of-charge estimation in the battery degradation process," *Applied Energy*, vol. 121, pp. 20–27, 2014.

[14] B. Cheng, Z. Bai, and B. Cao, "State of charge estimation based on evolutionary neural network," *Energy Conversion and Management*, vol. 49, no. 10, pp. 2788–2794, 2008.

[15] Q.-S. Shi, C.-H. Zhang, and N.-X. Cui, "Estimation of battery state-of-charge using ν-support vector regression algorithm," *International Journal of Automotive Technology*, vol. 9, no. 6, pp. 759–764, 2008.

[16] S. Zhang, L. Yang, X. Zhao, and J. Qiang, "A GA optimization for lithium-ion battery equalization based on SOC estimation by NN and FLC," *International Journal of Electrical Power and Energy Systems*, vol. 73, pp. 318–328, 2015.

[17] L. Zhao, M. Lin, and Y. Chen, "Least-squares based coulomb counting method and its application for state-of-charge (SOC) estimation in electric vehicles," *International Journal of Energy Research*, vol. 40, no. 10, pp. 1389–1399, 2016.

[18] W. Waag and D. U. Sauer, "Adaptive estimation of the electromotive force of the lithium-ion battery after current interruption for an accurate state-of-charge and capacity determination," *Applied Energy*, vol. 111, pp. 416–427, 2013.

[19] Z. Shen and C. D. Rahn, "Model-based state-of-charge estimation for a valve-regulated lead-acid battery using linear matrix inequalities," *Journal of Dynamic Systems, Measurement, and Control*, vol. 135, no. 4, Article ID 041015, 8 pages, 2013.

[20] M. Charkhgard and M. H. Zarif, "Design of adaptive H_∞ filter for implementing on state-of-charge estimation based on battery state-of-charge-varying modelling," *IET Power Electronics*, vol. 8, no. 10, pp. 1825–1833, 2015.

[21] A. Alfi, M. Charkhgard, and M. H. Zarif, "Hybrid state of charge estimation for lithium-ion batteries: design and implementation," *IET Power Electronics*, vol. 7, no. 11, pp. 2758–2764, 2014.

[22] F. Zhang, G. Liu, and L. Fang, "A battery state of charge estimation method using sliding mode observer," in *Proceedings of the 7th World Congress on Intelligent Control and Automation (WCICA '08)*, pp. 989–994, Chongqing, China, June 2008.

[23] M. Gholizadeh and F. R. Salmasi, "Estimation of state of charge, unknown nonlinearities, and state of health of a lithium-ion battery based on a comprehensive unobservable model," *IEEE Transactions on Industrial Electronics*, vol. 61, no. 3, pp. 1335–1344, 2014.

[24] B. Xia, C. Chen, Y. Tian, W. Sun, Z. Xu, and W. Zheng, "A novel method for state of charge estimation of lithium-ion batteries using a nonlinear observer," *Journal of Power Sources*, vol. 270, pp. 359–366, 2014.

[25] Y. Tian, B. Xia, M. Wang, W. Sun, and Z. Xu, "Comparison study on two model-based adaptive algorithms for SOC estimation of lithium-ion batteries in electric vehicles," *Energies*, vol. 7, no. 12, pp. 8446–8464, 2014.

[26] I.-S. Kim, "A technique for estimating the state of health of lithium batteries through a dual-sliding-mode observer," *IEEE Transactions on Power Electronics*, vol. 25, no. 4, pp. 1013–1022, 2010.

[27] B. Ning, J. Xu, B. Cao, B. Wang, and G. Xu, "A sliding mode observer SOC estimation method based on parameter adaptive battery model," *Energy Procedia*, vol. 88, pp. 619–626, 2016.

[28] F. Zhong, H. Li, S. Zhong, Q. Zhong, and C. Yin, "An SOC estimation approach based on adaptive sliding mode observer and fractional order equivalent circuit model for lithium-ion batteries," *Communications in Nonlinear Science and Numerical Simulation*, vol. 24, no. 1–3, pp. 127–144, 2015.

[29] C. R. Gould, C. M. Bingham, D. A. Stone, and P. Bentley, "New battery model and state-of-health determination through subspace parameter estimation and state-observer techniques," *IEEE Transactions on Vehicular Technology*, vol. 58, no. 8, pp. 3905–3916, 2009.

[30] X. Chen, W. Shen, Z. Cao, and A. Kapoor, "Adaptive gain sliding mode observer for state of charge estimation based on combined battery equivalent circuit model," *Computers and Chemical Engineering*, vol. 64, pp. 114–123, 2014.

[31] D. Kim, T. Goh, M. Park, and S. W. Kim, "Fuzzy sliding mode observer with grey prediction for the estimation of the state-of-charge of a lithium-ion battery," *Energies*, vol. 8, no. 11, pp. 12409–12428, 2015.

[32] D. Kim, K. Koo, J. J. Jeong, T. Goh, and S. W. Kim, "Second-order discrete-time sliding mode observer for state of charge determination based on a dynamic resistance Li-ion battery model," *Energies*, vol. 6, no. 10, pp. 5538–5551, 2013.

[33] E. Kuhn, C. Forgez, P. Lagonotte, and G. Friedrich, "Modelling Ni-mH battery using cauer and foster structures," *Journal of Power Sources*, vol. 158, no. 2, pp. 1490–1497, 2006.

[34] B. L. Walcott and S. H. Zak, "State observation of nonlinear uncertain dynamical systems," *IEEE Transactions on Automatic Control*, vol. 32, no. 2, pp. 166–170, 1987.

[35] K. M. Tsang, L. Sun, and W. L. Chan, "Identification and modelling of Lithium ion battery," *Energy Conversion and Management*, vol. 51, no. 12, pp. 2857–2862, 2010.

[36] S. Liu, J. Jiang, W. Shi, Z. Ma, L. Y. Wang, and H. Guo, "Butler–volmer-equation-based electrical model for high-power lithium titanate batteries used in electric vehicles," *IEEE Transactions on Industrial electronics*, vol. 62, no. 12, 2015.